Sill Processes in the Saguenay Fjord

Jérôme Guay[1] Daniel Bourgault[1] Cynthia Bluteau[1]
Cédric Chavanne[1] Peter Galbraith[2] Louis Gostiaux [3]

[1]Intitut des Sciences de la Mer de Rimouski; Université du Québec à Rimouski;

[2]Institut Maurice-Lamontagne, Ministère des Pêches et Océans Canada;

[3]Laboratoire de Mécanique des Fluides et d'Acoustique ; École Centrale de Lyon

The Saguenay Fjord

The Saguenay Fjord is a 110 km long, 250 m deep (max depth) and 2 km wide (on average) multi-silled glacial valley. The fjord is located in subarctic eastern Canada and connects Saguenay River at its head with the St. Lawrence Estuary at its mouth. The bathymetry is characterized with 3 sills : a shallow 20 m deep sill at the mouth, an intermediate 60 m and a deep 120 m sill deep respectively 20 and 35 km landward.

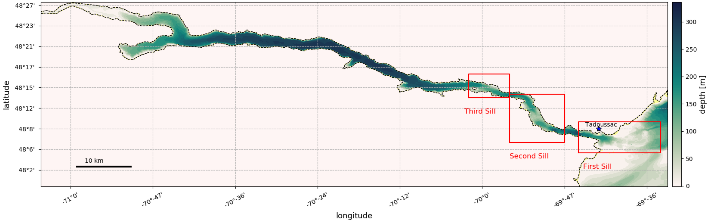

Fig. 1 – Map of the Saguenay fjord. Squared in red are the locations of each sill.

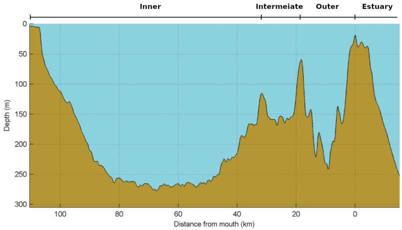

Fig. 2 – Longitudinal section of the fjord.

The sills separate the fjord into 3 basins : the outer, the intermediate and the inner basins.
The fjord's circulation is forced by freshwater input brought by the Saguenay River, large tides and wind.
The Saguenay river is the biggest fresh water contributor with an averaged discharge of 1200 m^3 s^{-1} (from 1944 to 1993)[Bélanger, 2003].
At the mouth, the tides reach 4 m and generated currents that can exceed 3 ms^{-1} [Stacey and Gratton, 2001].

Different circulation regimes have been identified in the fjord each renewing a different layer : deep, intermediate and subsurface([Belzile et al., 2016], [Galbraith, 2018]). Although it was initially believe that those regime were seasonally driven, we now know that they can occurs at different time in the year.

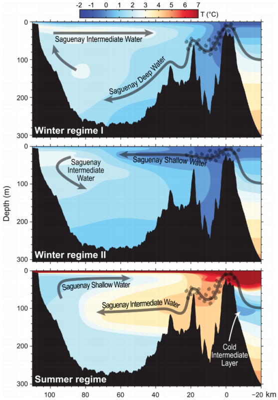

Fig. 3 – Schematic synthesis of the three seasonal renewal regimes in the Saguenay Fjord (Figure 13 of Belzile et al. [2016]). deep renewals during (top) fall and early winter, (middle) mid or late winter subsurface renewals, and (bottom) intermediate renewals during summer.

Motivations

Our research is motivated by indirect indications that those regimes are determined by turbulent processes occurring locally at each of these three sills. Here, we carried out a field experiment to more directly investigate the detailed dynamics of tidally-driven sill processes and water mass modifications occurring across these three sills.

Methodology

To observe the evolution of the flow over the different sills, a survey campaign was carried out in July 2018 aboard the R/V Coriolis II. The ship is equipped with ship mounted 4 beams 150 KHz ADCP and echo-sounder. Along-channel transect lines were defined over the second and third sills over which repeated transects were performed over complete tide cycles. Temperature/salinity data were sampled using a CTD probe mounted on a remote controlled oscillating towed fish.

Result

This presentation contains some observation made around the second and third sills with brief descriptions of the different phenomena.

Second Sill

During flood tide no internal hydraulic jump is generated as opposed to ebb tide. The internal hydraulic jump, located 1500 m seaward reaches about 60 m height. The strong traverse currents on the seaward side of the sill during ebb tide are a result of the transect line not being perpendicular to the sill's slope.

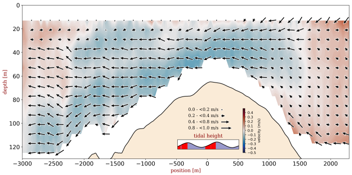

(a) Flood tide averaged

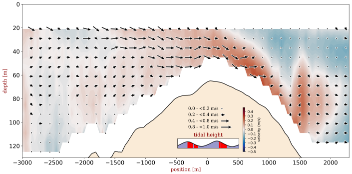

(b) Ebb tide averaged

Fig. 4 – The velocity fields were averaged over selected transects (red patches on the tide gauge). The quiver plot shows the along-track current. The colormap shows the transverse current with positive values indicating outward current.

Although the is no internal hydraulic jump during ebb tide, we see that there is more kinetic energy compared to flood tide. We therefore cannot assume that the lack of internal hydraulic jump is caused by the weaker currents. We also have to note that there is a significant part of the velocity field missing near the bottom which could hide current velocity greater than 1 m/s.

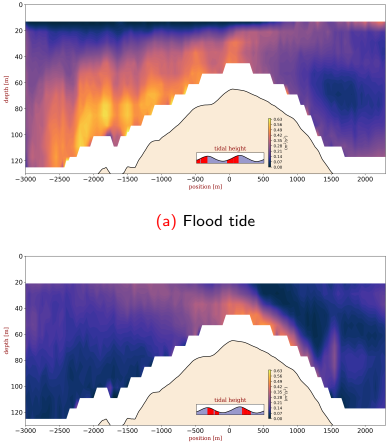

(a) Flood tide

(b) Ebb tide

Fig. 5 – The kinetic energy per mass fields were averaged over selected transects (red patches on the tide gauge). The selected transect time are shown on the tide gauge with red patches.

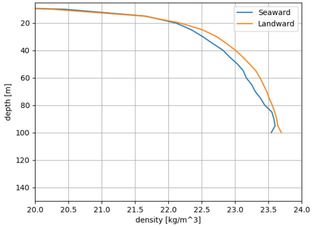

Fig. 6 – Averaged density profiles for a complete tide cycle. Standard deviation still need to be added.

When averaging profiles landward together and then seaward over a complete tidal cycle we see that there is slightly denser water landward of the sill crest. We hypothesize that the present of denser water is in part responsible for the lack of internal hydraulic jump during flood tide. A phenomena that may be similar to that documented by Klymak and Gregg [2003] in Knight Inlet (British Columbia, Canada).

On transect 42, half way through ebb tide, we clearly see on the acoustic image a gravity current along the seaward face of the sill fallowed by a internal hydraulic jump at 1500 m. The along-track velocity field and the density profiles also show the hydraulic jump but also the presence a weakly stratified layer with weak currents. This is a similar dynamic to what has been documented in Knight inlet by Farmer and Armi [1999].

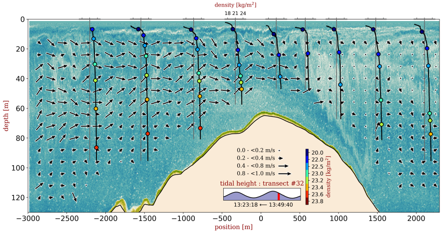

Fig. 7 – Transect number 42 over the second sill. The blue colormap shows the acoustic image. Along-track current is shown with arrows. Density profiles are shown in black. The colored dots highlight the isopycnals σ_t = 20, 22, 22.5, 23, 23.4, 23.6, and 23.8.

In early march 2020, sampling was carried out with a CTD probe on the landward side of the sill during ebb tide. The objective was to compare winter and summer internal hydraulic jumps. We here show that during winter time, the internal hydraulic jump occurs 400-500 m further down stream of the sill crest compare the summer time. Analyse of density overturns still need to be done to evaluate the kinetic energy dissipation rate.

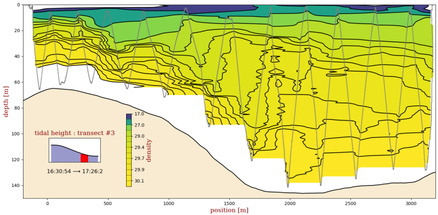

Fig. 8 – Third transect over the second sill during winter time. The isopycnal $\sigma_t = 17, 27, 29, 29.4, 29.7, 29.9$ and 30.1 are shown with a contour plot. The gray line shows the probe course during the sampling.

Internal waves are being generated at the sills between depth of 5 to 20 m during ebb tide.

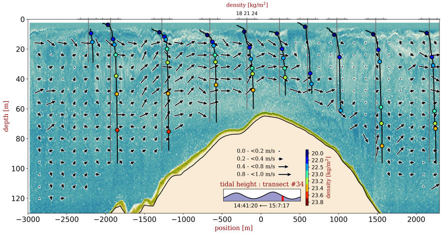

Fig. 9 – Transect number 34 over the second sill. The blue colormap shows the acoustic image. Along-track current is shown with arrows. Density profiles are shown in black. The colored dots highlight the isopycnals σ_t = 20, 22, 22.5, 23, 23.4, 23.6, and 23.8.

Example of the dynamic during flood tide. We can see strong current, between 0.8 and 1.0 m/s on the landward face of the sills.

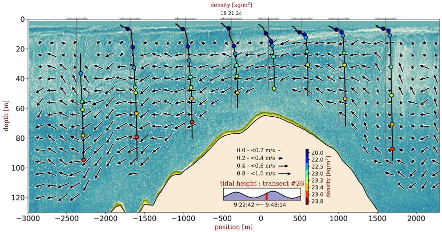

Fig. 10 – Transect number 23 over the second sill. The blue colormap shows the acoustic image. Along-track current is shown with arrows. Density profiles are shown in black. The colored dots highlight the isopycnals $\sigma_t = 20, 22, 22.5, 23, 23.4, 23.6$, and 23.8.

On transect 23, we are on early ebb tide. About 2000 m landward and at 100 m depth, there is a flow separation which may be caused by the presence of denser water landward of the sill crest.

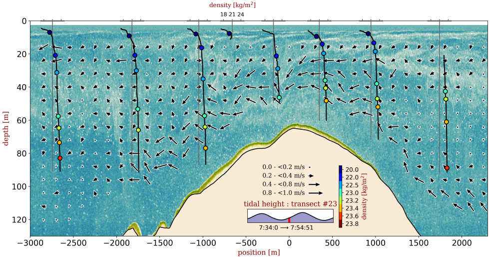

Fig. 11 – Transect number 26 over the second sill. The blue colormap shows the acoustic image. Along-track current is shown with arrows. Density profiles are shown in black. The colored dots highlight the isopycnals σ_t = 20, 22, 22.5, 23, 23.4, 23.6, and 23.8.

Third Sill

At the third sill, the currents are significantly weaker compared to the second sill. There is also no sign of a internal hydraulic jump during flood or ebb tide.

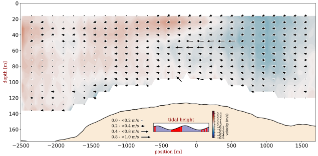

(a) Flood tide averaged

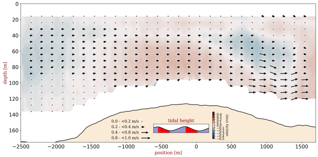

(b) Ebb tide averaged

Fig. 12 – The velocity fields were averaged over selected transects (red patches on the tide gauge). The quiver plot shows the along-track current. The colormap shows the transverse current with positive values indicating outward current.

When looking the kinetic energy, there is no difference in amplitude between flood and ebb tide. But compared to the second sill, there is about half as much kinetic energy.

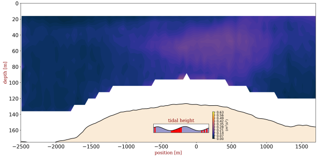

(a) Flood tide

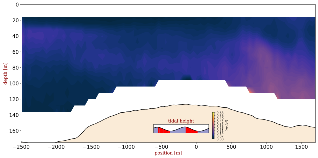

(b) Ebb tide

Fig. 13 – The kinetic energy per mass fields were averaged over selected transects (red patches on the tide gauge). The selected transect time are shown on the tide gauge with red patches.

Example of the dynamic during flood tide.

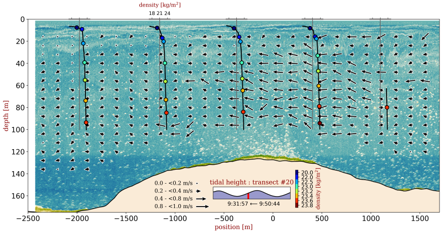

Fig. 14 – Transect number 20 over the third sill. The blue colormap shows the acoustic image. Along-track current is shown with arrows. Density profiles are shown in black. The colored dots highlight the isopycnals $\sigma_t = 20$, 22, 22.5, 23, 23.4, 23.6, and 23.8.

Example of the dynamic during ebb tide.

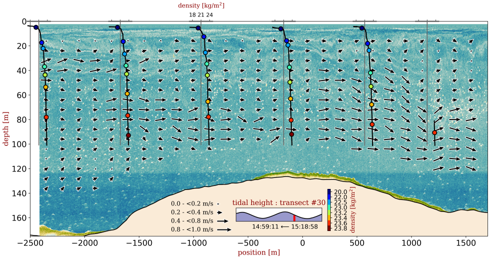

Fig. 15 – Transect number 30 over the third sill. The blue colormap shows the acoustic image. Along-track current is shown with arrows. Density profiles are shown in black. The colored dots highlight the isopycnals $\sigma_t = 20, 22, 22.5, 23, 23.4, 23.6$, and 23.8.

Perspective

Work is still ongoing to give better description of the sill processes in the Saguenay Fjord.

I'm looking forward to discuss the results and read your comments during the chat session.

Thank you,

Jérôme Guay

Bibliography

Bélanger, C. (2003). *Observation and modelling of a renewal event in the Saguenay Fjord*. PhD thesis, Université du Québec à Rimouski.

Belzile, M., Galbraith, P. S., and Bourgault, D. (2016). Water renewals in the saguenay fjord. *Journal of Geophysical Research : Oceans*, 121(1) :638–657.

Farmer, D. and Armi, L. (1999). Stratified flow over topography : the role of small-scale entrainment and mixing in flow establishment. *Proceedings of the Royal Society of London. Series A : Mathematical, Physical and Engineering Sciences*, 455(1989) :3221–3258.

Galbraith, Peter ; Bourgault, D. . B. M. (2018). Circulation et renouvellement des masses d'eau du fjord du saguenay. *Le Naturaliste canadien*, 142(2) :36–46.

Klymak, J. M. and Gregg, M. C. (2003). The role of upstream waves and a downstream density pool in the growth of lee waves : Stratified flow over the knight inlet sill. *Journal of physical oceanography*, 33(7) :1446–1461.

Stacey, M. W. and Gratton, Y. (2001). The energetics and tidally induced reverse renewal in a two-silled fjord. *Journal of Physical Oceanography*, 31(6) :1599–1615.